ITERATIVE ICI CANCELLATION BASED ON FACTOR GRAPHS FOR LARGE FFT SIZES

Pello Ochandiano†, Henk Wymeersch∗, Mikel Mendicute†, Lorena Martínez†, and Iker Sobron†

† Signal Theory and Communications Area
Electronics and Computing Department
University of Mondragon
Loramendi, 4, 20500 Mondragon, Spain
e-mail: pochandiano@eps.mondragon.edu

∗ Communications Systems and Information Theory Division
Department of Signals and Systems
Chalmers University of Technology
SE-412 96 Gothenburg, Sweden
e-mail: henkw@chalmers.se

ABSTRACT

This paper focuses on the challenging problem of signal reception for orthogonal frequency division (OFDM) systems in high mobility environments. A novel framework based on the well-known belief propagation (BP) algorithm is proposed for joint inter-carrier interference (ICI) cancellation, signal detection and channel decoding. The performance of the mentioned near-optimal detection strategy is analyzed over a general bit-interleaved coded modulation (BICM) system applying low-density parity-check (LDPC) codes. The inclusion of pilot symbols is also considered to analyze how they assist the detection process. A full parallel turbo receptor is derived which shows good performance when the ICI power is high due to high mobility or the use of large FFT sizes.

1. INTRODUCTION

Commercial requirements based on the demand of higher data rates, greater spectral efficiencies and improved data integrity have triggered the specification of recent broadband high speed communications standards. This is the case of IEEE's 802.16 family, the long-term evolution (LTE) project, or the recently standardized second generation digital video broadcasting (DVB) specifications. Mobility support is one of the key features of these new technologies, dealing with the challenge of enabling mobile broadband services at high vehicular speeds. Either the second generation DVB standards, with both terrestrial (DVB-T2) and handheld (DVB-NGH) versions, or the IEEE 802.16m are good examples of the mobility requirements of new wireless communication standards.

OFDM has been adopted by most of these new communication systems as modulation technique, since it has been shown to be a good candidate to overcome inter-symbol interference (ISI) caused by frequency-selective channels. In order to increase spectral efficiency or to allow the deployment of single-frequency networks (SFN), new large OFDM symbol lengths are being included in the latest standards (e.g., "32K" in DVB-T2).

Nevertheless, it is well known that one of the drawbacks of OFDM is its susceptibility to Doppler frequency shifts, which gives rise to so-called inter-carrier interference and deteriorates severely the bit error rate (BER) performance. The effect of ICI becomes critical when densely spaced subcarriers are used, so it becomes necessary to develop a reception strategy to solve the mobility-induced ICI problem.

Many different approaches have been studied with the aim of overcoming the issue of BER performance loss due to the presence of ICI: zero-forcing [1][2], minimum mean square error minimization [3][4], serial interference cancellation (SIC) [5], self-ICI cancellation [6], parallel interference cancellation (PIC) [7], maximum a-posteriori detection [8][9] or sphere decoding [10]. Regarding the way that ICI is considered, either as interference or as source of frequency diversity, there could be stated a difference between ICI suppressing schemes and complex detectors, respectively. The former try to subtract out the interference from the signal [11], while the latter exploit the frequency diversity introduced by the ICI in the OFDM symbol [9].

Peng and Ryan [11] suggest a parallel implementation of a two-stage equalizer, suitable for large FFT sizes but which suffers for performance loss at high Doppler frequencies. In [9], Liu and Fitz present a near-optimal reduced complexity MAP equalizer employing Bahl-Cocke-Jelinek-Raviv (BCJR) algorithm which achieves performance of free-ICI with normalized Doppler frequencies (f_d) up to 0.246 for 16QAM constellation, and analyze its application to the IEEE 802.16e mobile WIMAX standard. Nevertheless, this approach turns out to be inappropriate for some wireless communication systems with large OFDM symbol lengths (e.g., recent DVB standards) due to its intrinsic serial structure.

In recent years, graphical models, especially factor graphs (FG), have attracted the attention of many authors for representing the factorization of global functions. In this paper, we consider the application of this framework to detection over an ICI channel. We analyze the performance of the BP detector over a general bit-interleaved LDPC coded modulation (BILCM) communication system by performing joint, iterative detection and channel decoding through the exchange of soft information over a FG. Moreover, a general FG taking into account both the detection and decoding process is derived allowing fully parallel high-speed turbo reception, which makes it a very suitable receiver for the aforementioned last generation communication standards. Furthermore, pilot-assisted detection is also considered in the proposed BP scheme.

2. SYSTEM DESCRIPTION

OFDM modulation divides a data stream with sample period T into N substreams, which are modulated on different subcarriers, equally spaced at a distance of $\Delta_f = 1/(TN)$. This is achieved by transforming the set of N coded

frequency-domain symbols $\mathbf{s} = [s_1 ... s_N]^T$, equally likely and chosen from a complex constellation χ, into the time domain through an inverse discrete Fourier transform (IDFT) block. A cyclic-prefix (CP) of length G is added at the output of the IDFT. Assuming that the CP is longer than the channel delay spread, there is no inter-block interference (IBI) and the detector can be designed separately for each OFDM block. The received signal after CP removal may be written in matrix form as [4, eq.(1)]

$$\mathbf{r} = \overline{\mathbf{H}}\mathbf{F}^H\mathbf{s} + \mathbf{z}, \tag{1}$$

where $\overline{\mathbf{H}}$ is a $N \times N$ time-domain channel matrix, $\mathbf{F}^H$ stands for the standard N-point DFT matrix, and vectors $\mathbf{r}$ and $\mathbf{z}$ are the received signal and the AWGN discrete samples respectively. We assume that $\mathbf{z}$ is a complex Gaussian noise vector with zero mean and covariance $E\left\{\mathbf{z}\mathbf{z}^H\right\} = \sigma_n^2\mathbf{I}_N$.

At the receiver, after CP removal and discrete Fourier transform (FFT) operation, the output vector can be expressed as

$$\begin{aligned}\mathbf{y} =& \mathbf{F}\overline{\mathbf{H}}\mathbf{F}^H\mathbf{s} + \mathbf{F}\mathbf{z} \\ =& \mathbf{H}\mathbf{s} + \mathbf{z}_f,\end{aligned} \tag{2}$$

where $\mathbf{H} = \mathbf{F}\overline{\mathbf{H}}\mathbf{F}^H$ is the frequency-domain channel matrix, and $\mathbf{z}_f = \mathbf{F}\mathbf{z}$ is the frequency-domain noise vector which has the same statistics of time-domain noise $\mathbf{z}$. Note that $\mathbf{y} = \mathbf{F}\mathbf{r}$.

When the channel is time-invariant the frequency-domain channel matrix $\mathbf{H}$ is diagonal. However, in a time-varying channel, the ICI leads to off-diagonal elements of $\mathbf{H}$, which makes the implementation of conventional equalizers prohibitively complex. Since we know that most of the energy of the frequency channel matrix is concentrated in the vicinity of the diagonal, we can make use of the banded structure of $\mathbf{H}$ to design low-complexity detectors. We introduce a trade-off variable q as the number of diagonals to be taken into account as shown in Fig. 1. The higher the vehicular speed, or the larger the OFDM symbol, the higher has to be q to achieve the same BER. Nevertheless, for many applications, considering one neighboring subcarrier ($q = 3$) is enough to achieve good BER performance in relatively high mobility scenarios. Hence, $q = 3$ has been adopted as a reference in this research work.

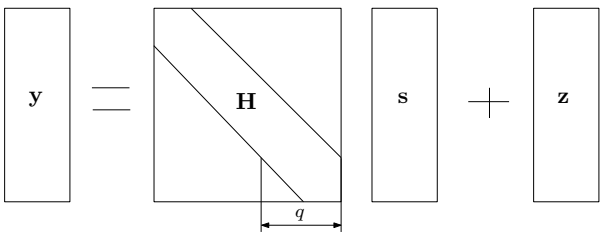

Figure 1: System input-output relation after removing the CP.

BP detector's performance is evaluated over a BICM scheme (Fig. 2) with the 64800 bits-long LDPC codes adopted by DVB [12]. We consider ideal channel state information (CSI) and perfect synchronization at the receiver. Even so, the presence of pilot carriers, widely used in communication systems for channel estimation, has been considered with the aim of analyzing how they can assist the BP detection process. The DVB-T2 PP1 pilot pattern [12] has been adopted for this purpose.

3. BELIEF PROPAGATION DETECTOR

Based on Bayesian estimation theory, it is well known that the transmission of a random signal over an AWGN-affected random channel, can be modeled

$$P(\mathbf{s}|\mathbf{y}) \propto P(\mathbf{y}|\mathbf{s})\,P(\mathbf{s}), \tag{3}$$

where $P(\mathbf{s}|\mathbf{y})$ denotes the joint a-posteriori distribution of $\mathbf{s}$, $P(\mathbf{y}|\mathbf{s})$ represents the likelihood function, and $P(\mathbf{s})$ is the a-priori distribution of $\mathbf{s}$. In order to compute the marginal $\{P(s_n|\mathbf{y})\}$, we can avoid the cumbersome evaluation of the joint a-posteriori APP function factorizing it into N factors. In case of a received signal affected by ICI and considering $q = 3$, this factorization can be expressed as

$$P(\mathbf{y}|\mathbf{s}) \propto \prod_{k=1}^{N} f_k(s_{k-1}, s_k, s_{k+1}), \tag{4}$$

where implicitly $s_k = 0$ for $k \leq 0$ and $k > N$ and

$$\begin{aligned}f_k(s_{k-1}, s_k, s_{k+1}) =& P(y_k|s_{k-1}, s_k, s_{k+1}) \\ &\propto \exp\left\{-\frac{\left|y_k - \sum_{i=k-1}^{k+1} H_{ki}s_i\right|^2}{N_0}\right\}.\end{aligned} \tag{5}$$

The factor graph for the above factorized function is depicted within the dashed box on the top side of Fig. 3. Operating on this graph, the sum-product (SP) algorithm allows to compute marginals in a computationally efficient way exchanging messages between factor and variable nodes. For numerical stability reasons log-domain SP has been implemented. Denoting by $\mu_{s\to f}(s)$ the message sent from a variable node s to a factor node $f(\psi)$ in log domain, where ψ is the set of variables arguments of f, and by $\mu_{f\to s}(s)$ the message in the opposite direction, being $\vartheta(v)$ the set of neighbors of a given node v, the message computation in variable and factor nodes respectively becomes

$$\mu_{s\to f}(s) = \sum_{h\in\vartheta(s)\setminus\{f\}} \mu_{h\to s}(s) \tag{6}$$

$$\mu_{f\to s}(s) = \sum_{\sim\{s\}} \exp\left[\ln f(\psi) + \sum_{z\in\vartheta(f)\setminus\{s\}} \mu_{z\to f}(z)\right]. \tag{7}$$

From Fig. 3, it is obvious that the FG representing the detector has girth 4, which means that the shortest cycle in the graph is length 4. It is well-known that marginals obtained in a loopy FG are not true marginal a-posteriori distributions, and it is in general hard to state whether the marginals converge to a reasonable distributions or not. Moreover, in many applications, the BER performance degradation due to the presence of short cycles has reduced the interest in FG-based approaches. In other cases, extensive simulation results have shown that even length 4 cycles do not pose significant problems in terms of BER [13]. Simulation results provided in this paper show that the proposed BP detector performs close to the cycle-free BCJR in terms of BER.

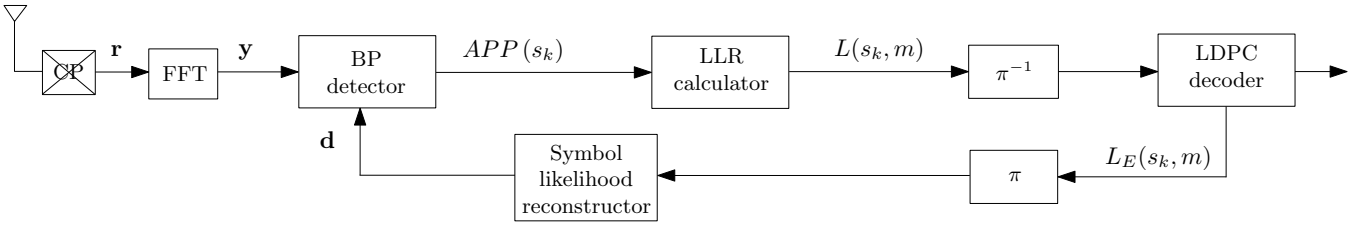

Figure 2: Block diagram of the BICM iterative reception chain including the proposed ICI canceling belief propagation detector.

After a fixed amount of iterations, the marginal APPs are calculated as follows,

$$APP(s_k) = \sum_{h \in \vartheta(s)} \mu_{h \to s}(s). \tag{8}$$

3.1 Pilot processing

Many communication systems use training data sequences with the aim of estimating the channel impulse response on the reception side. This information can be exploited to improve the performance of the receiver by performing the detection before removing the pilots. Fig. 3 describes how to deal with pilot carriers in the message passing process, where colored factor and variable nodes represent pilot carriers.

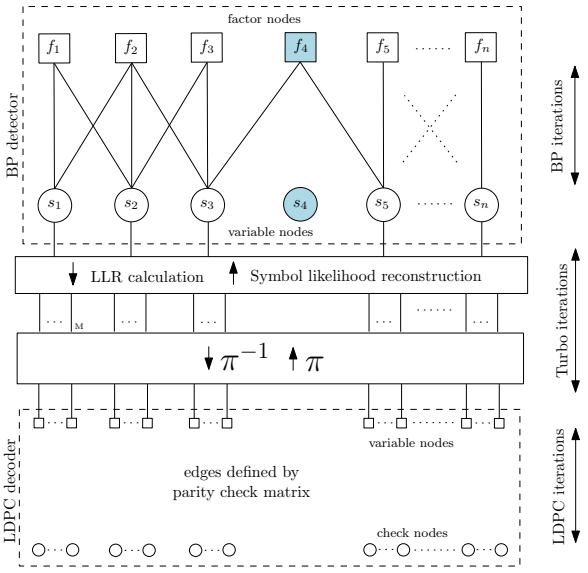

Figure 3: FG representing iterative joint data detection and decoding.

Message calculation in colored factor nodes takes into account that the transmitted symbol s_k is perfectly known, so that outgoing messages from these factor nodes are more accurate representations of the marginal distributions. On the other hand, regarding colored variable nodes, we can consider them as idle nodes, they do not exchange messages. As a consequence, some cycles are automatically removed from the FG. As an example, considering PP1 pilot pattern of DVB-T2 where pilot carriers represent the 8% of the total carriers, 8% of length 4 cycles are straightfowardly removed, which yields an additional BER improvement.

Flooding schedule is adopted as message-passing schedule where all variable and factor nodes pass new messages to their neighbors. As it is obvious, this schedule is the best suited for a parallel implementation of the receiver.

3.2 Turbo reception

Following the recent trend to design soft receptors enabling joint data detection and decoding, we have developed an iterative receptor which makes use of the extrinsic information generated by the LDPC decoder as a priori information at the detection process (Fig. 2). Based on the extrinsic LLRs at the output of the decoder $L_E(s_k,m)$, a priori symbol likelihoods $\mathbf{d}$ are reconstructed in order to inject reliable information in the variable nodes of the detection FG.

Considering that LDPC codes are decoded using FG-based algorithms, the joint data detection and decoding process can be depicted by a higher-order FG which shows the fully parallel structure of the proposed receptor (Fig. 3). A triple iterative scheme is proposed where messages are exchanged among internal LDPC decoder nodes (LDPC iterations), among internal decoder nodes (BP iterations), and between the detector and the decoder (turbo iterations) (Fig. 3).

3.3 Complexity analysis

The implementation of the log-domain SP algorithm can be carried out using the Jacobian logarithm, which only requires of summary operations and the evaluation of a nonlinear function by means of a lookup table. The complexity of the proposed algorithm is mainly a function of the following parameters: constellation size (M), number of total subcarriers (N) and number of subcarriers considered for ICI compensation (q). The overall complexity scales as $\mathscr{O}(NqM^q)$. Obviously, the higher the amount of total iterations is, the higher is the total complexity of the whole reception process. Therefore, it is necessary to choose the most efficient turbo schedule in order to reach a reasonable performance/complexity trade-off.

Regarding the BCJR algorithm, the computation of $M^{div(q,2)+1}$ values of the propagating message in the forward and backward recursions, requires summary operations involving M^q terms, whereas the computation of the marginal APP of s_k requires a summary operation involving M^q terms. div stands for integer division.

4. SIMULATION RESULTS

The performance of the proposed detection scheme is assessed by computer simulations in terms of BER versus SNR.

QPSK and 16QAM modulations are considered with the described BICM-OFDM system over the 6-taps Typical Urban (TU6) channel. The system bandwidth is 8 MHz and the carrier frequency is 760 MHz. Length 64800 extended irregular repeat-accumulate (eIRA) codes are implemented, with $2/3$ code rate (CR) for QPSK and $1/2$ for 16QAM, as well as the min-sum algorithm for its decodification. QPSK modulation is simulated for three mobile scenarios with $f_d = 0.13, f_d = 0.3$, and $f_d = 0.4$. The first one corresponds to about 200 km/h of vehicular speed for the 8K OFDM mode, and the last one represents about 120 km/h of vehicular speed for the 32K OFDM mode. On the other hand, $f_d = 0.22$ has been considered for 16QAM modulation, which corresponds to 350 km/h of vehicular speed for the 8K OFDM mode.

Extensive simulations have shown that performing 2 BP iterations and 20 LDPC iterations in each turbo iteration turns out to be a good turbo schedule in terms of complexity/performance trade-off. Therefore, this is the turbo schedule considered in this paper.

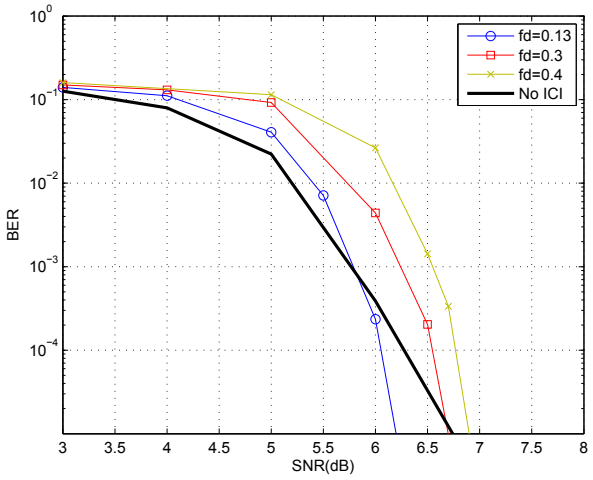

Figure 4: BER performance of turbo BP detector for QPSK constellation. 2 BP iterations and 20 LDPC iterations have been performed in each of the 5 turbo iterations.

First, we evaluate the aforementioned mobile scenarios for QPSK and compare the BER performance against the free-ICI case. Fig. 4 shows that even in the case of the highest Doppler frequency, BP detection outperforms the free-ICI case for low BER region. It is determined by simulations that the receptor approaches the convergence regime after 5 turbo iterations. Therefore, performing more turbo iterations does not imply significant BER performance gain.

We also appreciate that BP detector needs to overtake a minimum SNR bound to get to the water-falling region. Fig. 4 shows that this bound is higher for higher Doppler frequencies. The reason is that we consider just three subcarriers involved in ICI compensation, consequently we assume that there is a residual ICI described by the rest of the elements in matrix $\mathbf{H}$, whose power increases with f_d. Since we can consider this residual ICI Gaussian-like [14], the water-falling bound shifts to the right side in the SNR axis as f_d increases.

Performance of BP detector for QPSK is analyzed in more detail in Fig. 5 for $f_d = 0.4$. Turbo performance has been described depicting BER curves for different turbo iterations. The no-turbo case (10 BP iterations and 50 LDPC iterations) for $f_d = 0.4$ is also depicted in this figure in order to have a reference of how turbo scheme performs. We can appreciate that performing 2 turbo iterations is enough to outperform the no-turbo BP detection, which means that turbo scheme is more efficient in the sense that better BER performance is achieved with less amount of total iterations (both in the detector and the decoder). On the other hand, as previously stated, it is clearly shown that the turbo receptor tends to converge at about 5 iterations, giving rise to a performance gain of about 0.8 dB at BER=10^{-3} with respect to the no-turbo case.

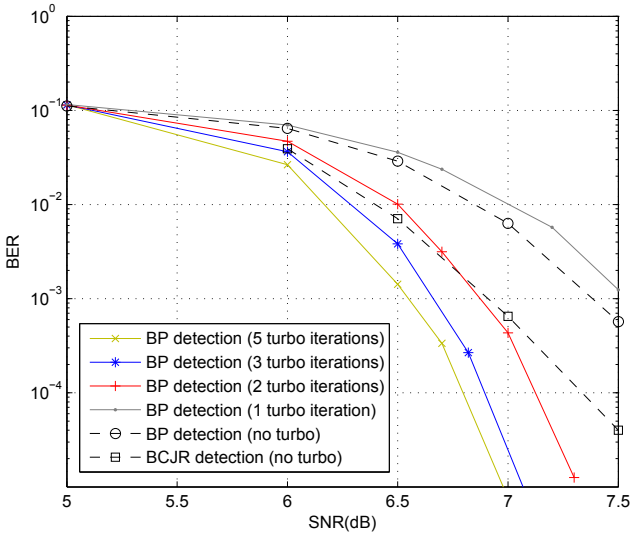

Figure 5: BER performance of turbo BP and BCJR detectors for QPSK constellation and $f_d = 0.4$. The no-turbo BP case performs 10 BP iterations and 50 LDPC iterations.

BCJR detector has also been considered with the aim of quantifying the performance loss due to the presence of short cycles in the FG. Comparing the no-turbo BCJR case with no-turbo BP detection, we can appreciate that our proposal is very closed to the optimal one (about 0.5 dB at BER=10^{-3}). Hence, although length 4 cycles exist, the APPs calculated by the BP are reliable enough to enable good ICI compensation. Moreover, there is a performance gain of about 0.3 dB at BER=10^{-3} between the turbo BP detector and the no-turbo BCJR. Note that turbo scheme has not been applied for BCJR since it is not feasible for large FFT sizes due to its intrinsic serial structure.

On the other hand, Fig. 6 shows the performance of the proposed detector for 16QAM. The BP detector is able to remove the error-floor caused by the Doppler frequency approaching the free-ICI case up to 2dB at BER=10^{-4}. BP detector does not achieve free-ICI performance for this Doppler frequency because the residual ICI affects much more higher order constellations. Considering 5 subcarriers involved in ICI would enhance the performance of BP detector, but this requires dealing with the complexity issue.

Comparing with BCJR, the complexity of FG-based detection algorithms can be reduced more efficiently since there is no constraint imposed by the trellis structure. Different approaches could be implemented in order to reduce the com-

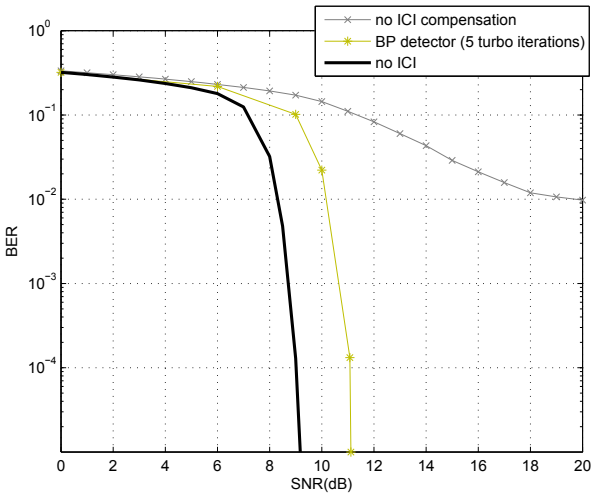

Figure 6: BER performance of turbo BP for 16QAM constellation and CR$= 1/2$. $f_d = 0.22$.

plexity of the proposed algorithm. Reduced-state sequence detection [15] also considered in [9] could be a good candidate for this purpose.

5. CONCLUSIONS AND FUTURE WORK

A novel FG-based detector has been proposed for wireless mobile OFDM systems which enables exploitation of the frequency diversity available in the received signal affected by ICI. The implementation of this novel scheme for signal detection allows high speed joint detection and decoding providing excellent performance at high mobility scenarios. The performance of the proposed detector has been analyzed over a TU6 channel model using LDPC codes. Furthermore, the inclusion of pilot symbols has also been considered in order to analyze how they can assist the detection process. Compared to the traditional BCJR receiver, the proposed FG detector is better suited to large FFT sizes. Future works will include exhaustive analysis of the iterative reception based on EXIT charts.

ACKNOWLEDGMENTS

The authors want to thank the Ministry of Industry, Tourism and Trade of the Spanish Government for funding the project FURIA 3 (TSI-020301-2009-33). They are additionally grateful to the Department of Industry and Innovation and to the Department of Education, Universities and Research of the Basque Government, for its support and funding through IKERTU programme.

REFERENCES

[1] J. Fu, C.-Y. Pan, Z.-X. Yang, and L. Yang, "Low-complexity equalization for TDS-OFDM systems over doubly selective channels," *IEEE Trans. on Broadcasting*, vol. 51, pp. 401–7, 2005.

[2] C.-Y. Hsu and W.-R. Wu, "Low-complexity ICI mitigation methods for high-mobility SISO/MIMO-OFDM systems," *IEEE Trans. on Vehicular Technology*, vol. 58, pp. 2755–68, 2009.

[3] X. Huang and H.-C. Wu, "Robust and efficient intercarrier interference mitigation for OFDM systems in time-varying fading channels," *IEEE Trans. on Vehicular Technology*, vol. 56, pp. 2517–28, 2007.

[4] K. Fang, L. Rugini, and G. Leus, "Low-complexity block turbo equalization for OFDM systems in time-varying channels," *IEEE Trans. on Signal Processing*, vol. 56, pp. 5555–66, 2008.

[5] S. U. Hwang, J. H. Lee, and J. Seo, "Low complexity iterative ICI cancellation and equalization for OFDM systems over doubly selective channels," *IEEE Trans. on Broadcasting*, vol. 55, pp. 132–9, 2009.

[6] C.-R. Sheu, M.-C. Tseng, C.-Y. Chen, and H.-P. Lin, "A low-complexity concatenated ICI cancellation scheme for high-mobility OFDM systems," *8th IEEE Wireless Communications and Networking Conference*, 2007.

[7] A. F. Molisch, M. Toeltsch, and S. Vermani, "Iterative methods for cancellation of intercarrier interference in OFDM systems," *IEEE Trans. on Vehicular Technology*, vol. 56, pp. 2158–2167, 2007.

[8] E. Panayirci, H. Dogan, and H. Poor, "A Gibbs Sampling Based MAP Detection Algorithm for OFDM over Rapidly Varying Mobile Radio Channels," *IEEE Global Telecommunications Conference*, 2009.

[9] D. Liu and M. Fitz, "Iterative MAP equalization and decoding in wireless mobile coded OFDM," *IEEE Trans. on Communications*, vol. 57, pp. 2042–51, 2009.

[10] Y. Liang, Q. Zhang, Z. Liu, F. Shu, and S. Berber, "Low-complexity sphere decoding for detection of OFDM systems in doubly-selective fading channels," *Elec. Letters*, vol. 45, pp. 797–8, 2009.

[11] F. Peng and W. Ryan, "A low-complexity soft demapper for OFDM fading channels with ICI," *IEEE Wireless Communications and Networking Conference*, pp. 1549–54, 2006.

[12] ETSI, "Digital Video Broadcasting (DVB); Frame structure channel coding and modulation for a second generation digital terrestrial television broadcasting system (DVB-T2). ETSI EN 302 755 V1.1.1," September 2009.

[13] M. Kaynak, T. Duman, and E. Kurtas, "Belief propagation over MIMO frequency selective fading channels," *2005 International Conference on Autonomic and Autonomous Systems*, 2005.

[14] T. Wang, J. Proakis, E. Masry, and J. Zeidler, "Performance degradation of OFDM systems due to Doppler spreading," *IEEE Trans. on Wireless Communications*, vol. 5, pp. 1422–32, 2006.

[15] M. Eyuboglu and S. Qureshi, "Reduced-state sequence estimation with set partitioning and decision feedback," *IEEE Trans. on Communications*, vol. 36, pp. 13–20, 1988.